# A Weighted Least Square Based Data Fusion Method for Precision Measurement of Freeform Surfaces

M.J. Ren[1], L.J. Sun[1], M.Y. Liu[2], C.F. Cheung[2], Y.H. Yin[1*]

[1]Robotics Institute, School of Mechanical Engineering, Shanghai Jiao Tong University, Shanghai, China

[2]Partner State Key Laboratory of Ultra-precision Machining Technology, Department of Industrial and Systems Engineering, The Hong Kong Polytechnic University, Kowloon, Hong Kong, China

[*]Corresponding author: yhyin@sjtu.edu.cn

**Abstract:** The trend towards product miniaturisation and multi-functionality constitutes a driving force for the application of complex surfaces in many fields such as advanced optics. The precision measurement of these surfaces should be carried out at multiple scales, of which process commonly involves several datasets obtained from different sensors. This paper presents a weighted least square based multi-sensor data fusion method for such measurement. The method starts from unifying the coordinate frames of the measured datasets using an intrinsic feature based surface registration method. B-spline surface is used to fit linear surface models to each identified overlapping area of the registered datasets, respectively. By forming a common basis function, the fitted surface models and the corresponding residuals of the datasets are then combined to construct a weighted least square based data fusion system which is used to generate a fused surface model with improved quality. An analysis of the uncertainty propagation in data fusion process is also given. Both computer simulation and actual measurement on a machined micro-structured freeform surface is conducted to verify the validity of proposed method, and the results indicate that the proposed method is capable of fusing multi-sensor measured datasets with notable reduction of measurement uncertainty.

**Keywords:** precision surface measurement, freeform surfaces, data fusion, weighted least square, B-spline

## 1. Introduction

The rapid development of the advanced machining technologies allows many complex components and devices to be manufactured with high precision [1-3]. The trend towards product miniaturisation has further driven the integration of micro scale features on macro scale components, and different scales of features are used to realize different functionality of products, for instance, in advanced optics and semiconductor. The measurement of these components requires to be carried out at multiple scales, which challenges current measurement technologies [4, 5].

Current measuring instruments can generally be divided into 5 categories [6-8], including coordinate measuring machines (CMM), topography measuring instruments, interferometric based instruments, scanning electron microscopy (SEM), and others, which cover a wide measurement range with high precision. Although these instruments have their own technical merits, no single instrument is able to fulfill all the required tasks and rendering multi-scale 3D measurement with nanometric accuracy. As a result, a sophisticated combination of several measuring techniques into a single system seems to be an appropriate solution for complex measurement tasks [9]. Multi-sensor techniques have already been utilized in precision surface measurement in recent years such as Werth VideoCheck UA 400 [10]. With the combination of several measuring sensors, these instruments are capable of performing measurement at multiple scales, and measuring complex 3D geometries with nanometric accuracy [9]. Data fusion is a further step after the multi sensor combination to produce a unique and improved output from the datasets measured by different sensors. In this process, the quality of the output largely depends on the data fusion method. This is due to the reason that, in multi sensor systems, the measured datasets may come from different spaces and time domains with different measurement principles, which imposes a lot of challenges to the fusion of these datasets for unique representation of the measured components. Although progress has been made in the multi-sensor instrumentation, there is still a lack of multi-scale modelling, analyzing, and fusion methods for the comprehensive characterization of the complex surfaces [4, 11].

Multi-sensor data fusion process involves two core steps including registration and fusion [9]. In registration, all the datasets are transformed to a common coordinate frame based on rigid motion. Iterative closest point (ICP) and its variants are the most widely used to methods in the registration of the discrete datasets [12, 13]. The method establishes the corresponding points of the two datasets which are used to determine the coordinate transformation matrix by minimizing the sum of the distances of the established corresponding pairs. The corresponding pairs of two datasets are iteratively decided by choosing the closest point. Due to the non-convexity of the optimization problem, the registration results may be trapped at a local minimum or even become divergent if the initial relative position of the two datasets is not provided appropriately [13]. Hence, a coarse registration is normally carried out to provide good initial values for the ICP iteration. Many coordinate transformation invariant surface features, such as local shape features [14] and curvature [15], and geometric moment [16], have been served as surface descriptors to aid the registration process. However, for the datasets registration in multi-sensor data fusion, most of these methods are difficult to be transferred since the surface descriptors are either susceptible to the shape of the datasets or not sufficiently representative for geometric details. This is due to the reason that, in multi-sensor system, the datasets only overlap certain amount to guarantee the measurement efficiency, and the registration would be false if the features are weak in the overlapping area.

Fusion is responsible for processing the redundant data in the overlapping area of the datasets so as to produce a unique representation. Although multi-sensor data fusion is widely used in the fields such as signal processing and image fusion, limited research work has been found in coordinate measurements. Wang et al. [4] recently gave a comprehensive literature review of multi sensor data fusion in surface topography measurement, and summarized the data fusion method into four categories, including repeated measurements, stitching, range image fusion, and 3D data fusion. In these categories, the 3D data fusion is the most difficult task which involves registration and fusion of complex surfaces, and tackles datasets on different scales. Ramasamy et al.

[17] presented several data fusion strategies to deal with measurement data from different magnifications in multi scale measurement using white light interferometer. However, the uncertainty propagation in fusion process is unclear. Gaussian process was recently applied in data fusion of coordinate datasets [18, 19]. The method establishes a Gaussian process model to describe the mean and the covariance function via Bayesian inference, and the fusion results are estimated based on maximum marginal likelihood estimation. The application of the method is still limited to relatively simple surfaces， and the time for the computation becomes infeasible when a large amount of data is involved. Forbes et al [20] presented a weighted least square based multi-sensor data fusion method which used a general Bayesian approach to balance the noise parameters by introducing weights to each datasets. Kalman filter [21] has similar fusion process with weighted least square method, but has superior efficiency when there are a lot of datasets to be fused. However, the methods rely on the fitting accuracy of the linear surface model, and have limited application in multi-sensor data fusion.

As a result, this paper presents a weighted least square based multi-sensor data fusion method for the measurement of freeform surfaces. To address the key problems in data fusion, an intrinsic feature based surface registration method is proposed to unify the coordinate frame of the measured datasets, and the B-spline surface is used to approximate each identified overlapping area of the registered datasets respectively based on a common basis function. The fitted surface models and corresponding residuals of the datasets are then combined to construct a weighted linear data fusion system which is used to generate a fused surface model with improved quality. Experimental work is presented to verify the effectiveness of the proposed method.

## 2. Weighted Least Square Based Data Fusion Method

### 2.1 Overview of the fusion method

Datasets measured by multi-sensor system may possess different resolutions, different levels of uncertainties, and embed in different coordinate systems. To address the key issues in data fusion, the proposed method performs the data fusion in three steps, including preprocessing, registration and fusion. Fig.1 shows the framework of the proposed method. In the first step, all the measured datasets are transferred into a common and appropriate representation format and filtering techniques are used to eliminate the outliers which may be included in each measured datasets. In the second step, an intrinsic feature based registration method is introduced to unify the coordinate frames of the measured datasets and to identify the overlapping areas among the datasets. In the third step, B-spline surface is used to fit a linear model to approximate the overlapping area of the datasets, and a weighted linear fusion system is established to fuse these datasets in a least square fashion.

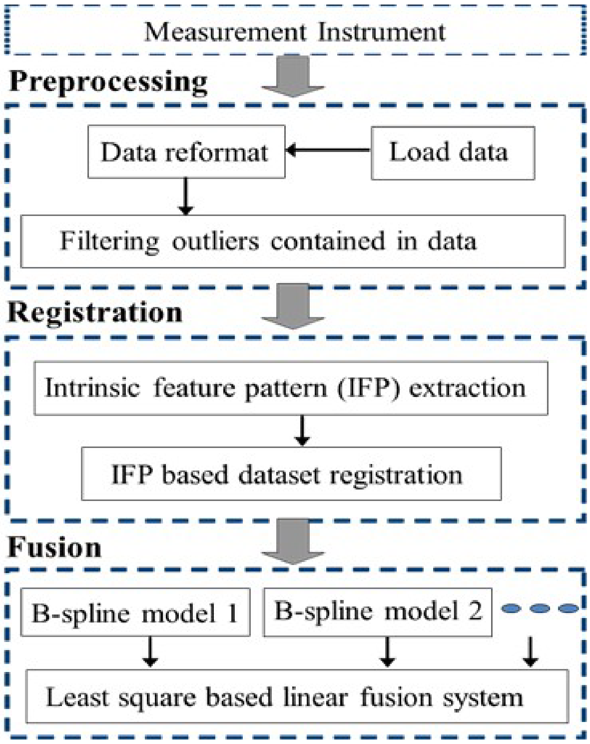


Fig. 1: Framework of Weighted Least Square Based Data Fusion Method

### 2.2 Intrinsic feature based data registration

Surface representation is the first step towards the goal of correspondence searching/surface registration. The commonly used freeform surface representation methods, such as parametric surfaces (e.g. NURBS) or points cloud, are highly dependent on the implicit parameterization and the embedded coordinate system, which leads difficulty in surface registration. In the present study, an intrinsic feature pattern (IFP) is used to represent the geometry of the measured datasets [15]. Surface intrinsic features refer to those surface features whose values are invariant under the transformation of the embedded coordinate frame and are free to the implicit parameterization of the surface. Taking Gaussian curvature as an example, it is an intrinsic property of a surface used to describe how "curve" is the surface, and is invariant under the transformation of the coordinate system.

Generally, there are two basic mathematical entities that are considered in the differential geometry of a surface $\boldsymbol{S}$, i.e. the first and second fundamental forms of a surface [22], as given by Eq. (1) and Eq. (2).

$$I = Edu^2 + 2Fdudv + Gdv^2 \tag{1}$$

$$II = Ldu^2 + 2Mdudv + Ndv^2 \tag{2}$$

where

$$E = \left(\frac{\partial \boldsymbol{S}(u,v)}{\partial u}\right)^2, \quad F = \frac{\partial \boldsymbol{S}(u,v)}{\partial u}\frac{\partial \boldsymbol{S}(u,v)}{\partial v}, \quad G = \left(\frac{\partial \boldsymbol{S}(u,v)}{\partial v}\right)^2$$

$$L = \frac{\partial^2 \boldsymbol{S}(u,v)}{\partial u^2}\cdot\frac{\boldsymbol{S}_u \times \boldsymbol{S}_v}{\left\|\boldsymbol{S}_u \times \boldsymbol{S}_v\right\|}, \quad M = \frac{\partial^2 \boldsymbol{S}(u,v)}{\partial u \partial v}\cdot\frac{\boldsymbol{S}_u \times \boldsymbol{S}_v}{\left\|\boldsymbol{S}_u \times \boldsymbol{S}_v\right\|}, \quad N = \frac{\partial^2 \boldsymbol{S}(u,v)}{\partial v^2}\cdot\frac{\boldsymbol{S}_u \times \boldsymbol{S}_v}{\left\|\boldsymbol{S}_u \times \boldsymbol{S}_v\right\|}$$

$(u,v)$ are the parameters of the surface $\boldsymbol{S}$.

The IFP representation is inspired from the uniqueness theorem proposed by Besl [22]. That is, if two surfaces possess same fundamental forms at every point on the surfaces, then they have the same shape. The theorem implies that an arbitrary smooth 3D surface shape is completely captured by six scalar functions, i.e. *E*, *F*, *G*, *L*, *M*, and *N*, i.e. an arbitrary smooth 3D surface can be uniquely represented by the six scalar functions. Although these scalar functions depend on the surface parameterization or the embedded coordinate frame, there are several combinations of these functions that yield specific features of surface shape, which are invariant surface features, such as Gaussian curvature and mean curvature as given by Eq. (3) and Eq. (4).

$$K = \det\left(\begin{bmatrix} E & F \\ F & G \end{bmatrix}^{-1}\right)\det\left(\begin{bmatrix} L & M \\ M & N \end{bmatrix}\right) \tag{3}$$

$$H = \frac{1}{2} tr\left(\begin{bmatrix} E & F \\ F & G \end{bmatrix}^{-1}\begin{bmatrix} L & M \\ M & N \end{bmatrix}\right) \tag{4}$$

where $\det(\cdot)$ and $tr(\cdot)$ denote the determinant and trance of a matrix, respectively. In the present study, Gaussian curvature and mean curvature are extensively used as intrinsic surface features for describing the surface geometry for generality and simplicity.

The main process of the method is as follows. A grid of points is sampled on each datasets and their curvatures are mapped to a 2D plane to form two bitmap images, respectively. This bitmap images are used to represent the geometry of the datasets. It is anticipated that the layout of a two dimensional texture onto a general surface inevitably creates distortion. Hence, in the present study, a spring mesh model [23] is used to fit the freeform surface such that the texture distortion of the mesh can be minimized by minimizing the spring energy of the model. An example of the IFP generation is given in Fig. 2.

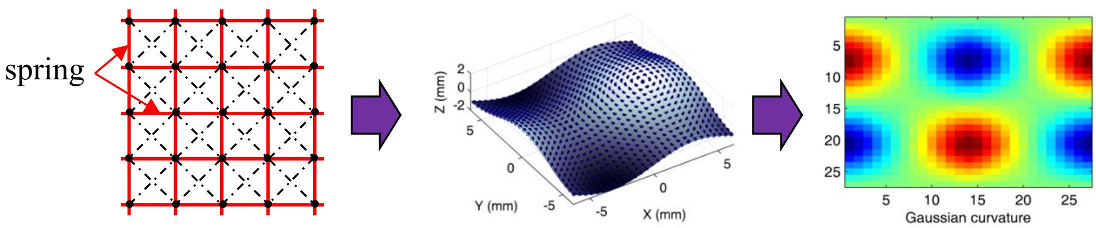


Fig. 2: Generation of invariant feature pattern

The surface registration problem is then converted to intrinsic feature pattern registration. That is, the corresponding searching is performed in 2D space rather than in 3D space. Registration problems involving translation and rotation are recovered by applying Fourier-Mellin transform and phase correlation method [24]. By registering two intrinsic feature patterns, point-to-point correspondence pairs are established between two surfaces. The established correspondence pairs can then be used to estimate the coordinate transformation of the two coordinate systems. There are several factors would influence the accuracy of the established correspondence by the proposed method including the texture distortion during the mapping, the error of the texture registration and so on. Hence, the established correspondence is considered as a result of semi-fine registration and is refined using ICP method [12]. The calculation of the intrinsic surface features like curvature is sensitive to the noise and the surface roughness contained in the measured data. Hence in practice, a proper smoothing should be conducted before the calculation of the curvature [25]. Furthermore, IFP is a kind of range image which composed of a set of curvatures of the surface. Even with certain level of noise, the robustness of the registration can well be maintained via the image registration process.

### 2.3 Weighted least square data fusion method

Fusion is responsible for producing a unique representation of the data at the overlapping area of the registered datasets, which can be casted as a regression problem of the form $\mathrm{Z(x)} = \mathrm{f(x)} + \varepsilon_m$, in which $\mathrm{Z(x)}$ are the measured data, "f( )" is an unknown model function which represents the shape of the datasets, $\varepsilon_m$ are the associated measurement error which are normally considered as identically distributed normal noise vector with $\varepsilon_m \sim N(0, \sigma_m I)$ for well calibrated instruments. The objective of the problem is to evaluate a putative form of "f( )" so that predictions can be made at arbitrary position over the measured area as accurate as possible. In the present study, linear model function is used to construct the fusion system so that:

$$\begin{bmatrix} \boldsymbol{Z}_1 \\ \boldsymbol{Z}_2 \\ \vdots \\ \boldsymbol{Z}_k \end{bmatrix} = \begin{bmatrix} \boldsymbol{C}_1 \\ \boldsymbol{C}_2 \\ \vdots \\ \boldsymbol{C}_k \end{bmatrix} \boldsymbol{\alpha} + \begin{bmatrix} \boldsymbol{\varepsilon}_{r1} \\ \boldsymbol{\varepsilon}_{r2} \\ \vdots \\ \boldsymbol{\varepsilon}_{rk} \end{bmatrix} \tag{5}$$

where $Z_i$ $(i = 1,2, \ldots, k)$ is the $i$th measured datasets; $C_i$ is the matrix of the $i$th dataset which arises from the model function; $\boldsymbol{\alpha}$ is the matrix of the unknown parameters of the model function; $\varepsilon_{ri}$ is the fitting residual error of the $i$th dataset. It is noted that $\varepsilon_{ri}$ is no longer the same as the $\boldsymbol{\varepsilon}_m$, but a combination of the fitting error and the measurement error since the fitting error is inevitable in actual measurement.

If $\varepsilon_{ri}$ is still a identically distributed normal noise vector with $\varepsilon_{ri} \sim N(0, \boldsymbol{\sigma}_{ri}\boldsymbol{I})$, the model parameter $\boldsymbol{\alpha}$ can be obtained by minimizing the following equation:

$$F = \frac{1}{2}(\boldsymbol{Z} - \boldsymbol{C\alpha})^T (\boldsymbol{Z} - \boldsymbol{C\alpha}) \tag{6}$$

where $\boldsymbol{Z} = [Z_1, Z_2, \ldots, Z_k]$, $\boldsymbol{C} = [\boldsymbol{C}_1, \boldsymbol{C}_2, \ldots, \boldsymbol{C}_k]$. Considering different fitting residuals $\varepsilon_{ri}$ would have different variances, weights can be given to each individual model based on its standard variance to eliminate the heteroscedasticity so that unbiased estimation can be achieved, as given in Eq. (7).

$$F = \frac{1}{2}\left(\boldsymbol{Z} - \boldsymbol{C\alpha}\right)^T \boldsymbol{W}\left(\boldsymbol{Z} - \boldsymbol{C\alpha}\right) \tag{7}$$

$$\boldsymbol{W} = \begin{bmatrix} \boldsymbol{w}_1 & & & \\ & \boldsymbol{w}_2 & & \\ & & \ddots & \\ & & & \boldsymbol{w}_k \end{bmatrix}$$

where $\boldsymbol{w}_i = diag[1/V_i^2, \dots, 1/V_i^2]$ is $dn_i \times dn_i$ matrix, $V_i$ is the variance of the fitting residual $\varepsilon_{ri}$, $dn_i$ is the number of the points contained in the $i$th dataset. $\boldsymbol{\alpha}$ can then be determined by vanishing the partial derivative of Eq. (7) to $\boldsymbol{\alpha}$ as follows.

$$\frac{\partial F}{\partial \boldsymbol{\alpha}} = \frac{\partial}{\partial \boldsymbol{\alpha}}\left(\frac{1}{2}\left(\boldsymbol{Z} - \boldsymbol{C\alpha}\right)^T \boldsymbol{W}\left(\boldsymbol{Z} - \boldsymbol{C\alpha}\right)\right) = 0 \tag{8}$$

$$\boldsymbol{\alpha} = \left(\boldsymbol{C}^T \boldsymbol{W} \boldsymbol{C}\right)^{-1} \boldsymbol{C}^T \boldsymbol{W} \boldsymbol{Z} \tag{9}$$

Obviously, the linear model forms the beating heart of the proposed method.

Due to the practically unlimited degree of geometric freedom and simple mathematics, B-spline surface is used to approximate the surface geometry. A B-spline surface $\boldsymbol{S}$ is defined as [26]:

$$\boldsymbol{S}(u,v) = \sum_{i=0}^{i=n_u-1} \sum_{j=0}^{j=n_v-1} N_{i,p}(u) N_{j,q}(v) \boldsymbol{P}_{ij} \tag{10}$$

where $\boldsymbol{P}_{i,j}$ is the control point controlling the shape of the surface; $n_u$ and $n_v$ are the numbers of control points; $u$ and $v$ are surface parameters identifying the location of point $\boldsymbol{S}$; $N_{i,p}(u)$ and $N_{j,q}(v)$ are the normalized B-spline functions uniquely defined by the degrees $(p, q)$ and knot vectors $(U, V)$ respectively. Eq. (10) can further be simplified to Eq. (11) as follows:

$$\boldsymbol{S}(u,v)=\sum_{s=0}^{n_c-1} N_s(u,v)\boldsymbol{P}_s \tag{11}$$

$$n_c = n_u n_v\,,\quad \boldsymbol{P}_s = \boldsymbol{P}_{i(s),j(s)}\,,\quad N_s(u,v) = N_{i(s),p}(u)N_{j(s),q}(v)$$

$$i(s)=\left\lfloor \frac{s}{n_v} \right\rfloor,\quad j(s)=s \bmod n_v$$

Substituting Eq. (11) to Eq. (5) and Eq. (9), a B-spline based linear fusion system can be constructed, and the control points of the fusion model can be evaluated as follows:

$$\tilde{\boldsymbol{P}}=\left(\boldsymbol{N}^T\boldsymbol{W}\boldsymbol{N}\right)^{-1}\boldsymbol{N}^T\boldsymbol{W}\boldsymbol{Z} \tag{12}$$

where $\boldsymbol{N}$ is $\sum_{i=1}^{k} dn_i \times n_c$ matrix of base function, $\widetilde{\boldsymbol{P}}$ is $n_c \times 3$ matrix of control points.. It is inferred from previous discussion that the effectiveness of the linear fusion system largely depends on the fitting quality of the model function. To obtain a best linear unbiased estimation of the model parameters, the fitted B-spline surface model should guarantee that the fitting residuals of each measured datasets can fairly be considered as identically distributed normal noise, and the variance of the residuals can also be used to design the weight for each dataset in fusion system.

In the present study, the quality of each individual fitting is controlled by enforcing a fitting error threshold which is given in accordance to the magnitude of the measurement error associated in the measured dataset. By enforcing the fitting error threshold, the individual fitting of each measured dataset is performed in such a way that the constructed models accurately represent the shapes of the datasets while the fitness can also be controlled as well to exclude the measurement noise from the model. In practice, it is almost impossible to guess number of the control points necessary to given fitting error threshold. As a result, the boundaries of the dataset are fitted to construct an initial surface which is used to assign good parameters values, i.e. $(u, v)$ in Eq. (10) to each point in the dataset, and to estimate the minimal degree of the freedom of the B-spline model, i.e. the number of the control points needed to characterize the shape of the dataset. Iteration process is then carried out to improve the fitting quality by increasing the number of the control points via knot insertion process.

In the construction of the linear fusion system, all the individual models must be made compatible by forming a common knot vector via knot insertion and removal of the knot vectors of the individual models. This is accomplished in three steps. Firstly, the B-spline model of the dataset with lower resolution is constructed. Secondly, the model of the dataset with higher resolution is constructed by taking the knot vector of the firstly constructed model as input. Lastly, the two knot vectors are made compatible via knot insertion of the prior knot vector. The process is continued upon processing all the datasets. To avoid the explosion of control points in constructing the linear fusion system, a candidate knot vector should also be passed in modelling each measured datasets. In this way, the generated common knot vector will ensure the number of the control points necessary for each individual fitting as well as for the linear fusion system.

## 2.4 Uncertainty analysis

The error associated in the measured datasets would inevitably propagate to the fusion results. In the present study, the knot vectors of the fused model are pre-determined from each individual fitting of the measured datasets, and the fusion process can be considered as a process of optimizing the distribution of the control points. Therefore the uncertainty propagation from the measured datasets to the fusion results can be determined by the covariance of the estimated model parameters, i.e. the control points $\boldsymbol{P}$ of the B-spline surface. The covariance of the $\boldsymbol{P}$ can be determined by Eq. (13) as follows:

$$\operatorname{cov}(\boldsymbol{P}) = E\left(\left(\boldsymbol{P}-\tilde{\boldsymbol{P}}\right)\left(\boldsymbol{P}-\tilde{\boldsymbol{P}}\right)^{T}\right) \tag{13}$$

where $\tilde{\boldsymbol{P}}$ is the best estimate of the $\boldsymbol{P}$ which is determined by Eq. (12) in previous section.

Left multiplying $(\mathrm{N^T WN})^{-1}(\mathrm{N^T WN})$ to P, the $(\mathrm{P}-\tilde{\mathrm{P}})$ is calculated as follows

$$\begin{aligned}\left(\boldsymbol{P}-\tilde{\boldsymbol{P}}\right) &= \left(\boldsymbol{N}^{T}\boldsymbol{WN}\right)^{-1}\left(\boldsymbol{N}^{T}\boldsymbol{WN}\right)\boldsymbol{P} - \left(\boldsymbol{N}^{T}\boldsymbol{WN}\right)^{-1}\boldsymbol{N}^{T}\boldsymbol{WZ} \\ &= \left(\boldsymbol{N}^{T}\boldsymbol{WN}\right)^{-1}\boldsymbol{N}^{T}\boldsymbol{W}\left(\boldsymbol{NP}-\boldsymbol{Z}\right) \\ &= \left(\boldsymbol{N}^{T}\boldsymbol{WN}\right)^{-1}\boldsymbol{N}^{T}\boldsymbol{W\varepsilon}\end{aligned} \tag{14}$$

where $\boldsymbol{\varepsilon}$ is the associated measurement error as given in Eq. (5). Substituting Eq. (14) to Eq. (13), the following preserve

$$\begin{aligned}\operatorname{cov}(\boldsymbol{P}) &= \left(\left(\boldsymbol{N}^{T}\boldsymbol{WN}\right)^{-1}\boldsymbol{N}^{T}\boldsymbol{W\varepsilon}\right)\left(\left(\boldsymbol{N}^{T}\boldsymbol{WN}\right)^{-1}\boldsymbol{N}^{T}\boldsymbol{W\varepsilon}\right)^{T} \\ &= \left(\boldsymbol{N}^{T}\boldsymbol{WN}\right)^{-1}\boldsymbol{N}^{T}\boldsymbol{W\varepsilon\varepsilon}^{T}\boldsymbol{WN}\left(\boldsymbol{N}^{T}\boldsymbol{WN}\right)^{-1}\end{aligned} \tag{15}$$

Considering the design of the weights as given in Eq. (7), Eq. (15) can further be simplified to

$$\operatorname{cov}(\boldsymbol{P}) = \left(\boldsymbol{N}^T\boldsymbol{W}\boldsymbol{N}\right)^{-1} \tag{16}$$

Therefore, the expectation and the variance of an arbitrary point S on the fused model can be determined based on the covariance of the control points, as given in Eq. (17) and Eq. (18).

$$E(\boldsymbol{S}) = \boldsymbol{N}\left(\boldsymbol{N}^T\boldsymbol{W}\boldsymbol{N}\right)^{-1}\boldsymbol{N}^T\boldsymbol{W}\boldsymbol{Z} \tag{17}$$

$$V(\boldsymbol{S}) = \boldsymbol{N}\left(\boldsymbol{N}^T\boldsymbol{W}\boldsymbol{N}\right)^{-1}\boldsymbol{N}^T \tag{18}$$

## 3. Experimental study

### 3.1 Computer simulation

To examine the performance of the proposed method, a sinusoidal freeform surface is designed as given by Eq. (8).

$$z = \sin(0.5x) + \cos(0.5y) \tag{19}$$

where $x, y \in [-2\pi, 2\pi]$ (unit in mm). A set of points is uniformly sampled on the entire surface with spacing 0.4 mm and is added Gaussian noise with standard deviation 5μm, and denoted as *D1*. Another set of points is sampled from a portion ($x, y \in [-\pi, \pi]$) of the designed surface with spacing 0.2 mm and is added Gaussian noise with standard deviation 15μm, and denoted as *D2*. *D2* is then moved to an arbitrary position so that the two datasets are no longer embedded into a common coordinate frame. Hence, the two datasets now possess different resolutions with different level of associated uncertainties and are embedded in different coordinate frames. Fig. 3 shows the produced *D1* and *D2* in a common coordinate frame.

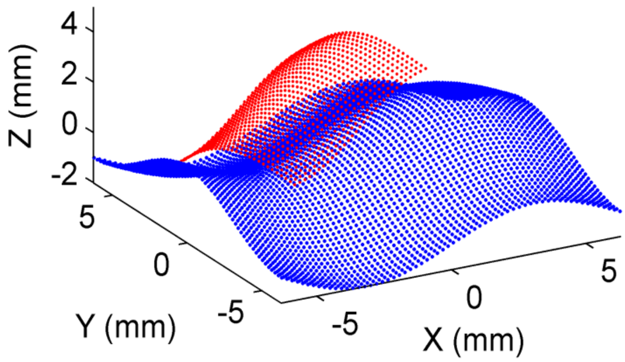


Fig. 3: Simulated multi-sensor datasets

The proposed method is then used to fuse the two datasets for producing a fusion dataset with improved quality. Firstly, intrinsic feature patterns are sampled from the two datasets. Image registration is then conducted to establish the correspondence between two datasets and identify the overlapping area, as shown in Fig. 4. Coordinate transformation is conducted to unify the coordinate frame of the two datasets. Secondly, at the identified overlapping area, B-spline surface is used to construct linear model to represent the geometry of the datasets. Finally, two established linear surface models are used to construct a weighted fusion system so as to fuse the two datasets based on the proposed method.

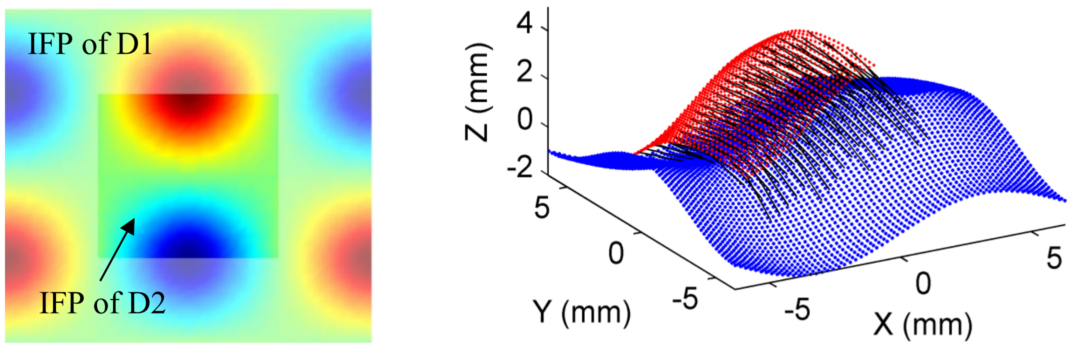


(a) IFP registration (b) correspondence establishment

Fig. 4: IFP based surface registration

The accuracy of the fusion results are characterized by the peak-to-valley error (PV) root-mean-square error (RMS) of reconstructed surface comparing with the theoretical designed surface. To analyse the robustness of the proposed method, a total of 100 simulations are conducted to study the effectiveness of the proposed fusion method. In each simulation, the RMS of the surface models of the datasets and the fused model are evaluated. A summary of the comparisons among the results are given in Table. 1. Comparing with the added errors, the RMS of the established B-spline models, i.e. the model 1 and model 2 are dramatically reduced to 2.1μm and 3.3μm respectively, as shown in Table 1. This is due to the reason that appropriate fitting error thresholds have been enforced to the individual fitting of each measured dataset so that the constructed models accurately represent the shapes of the datasets while the fitness can also be controlled as well to exclude the measurement noise from the model. In addition, much reduction has been found in model 2 comparing with model 1. This is due the reason that the model 2 contains more data than model 1 so that shrank uncertainty of the model parameters can be achieved. It is also seen from the results that RMS of the fused model is smaller than that of the lowest individual dataset. This implies that the proposed fusion method is capable of improving the fidelity of the reconstructed surface model via weighted fusion process.

Table 1: Error analysis of the surface model

| | Mean of RMS | Std of RMS | Mean of PV | Std of PV |
|---|---|---|---|---|
| **Model 1** | 2.1 µm | 0.13 µm | 15.7 µm | 2.3 µm |
| **Model 2** | 3.3 µm | 0.21 µm | 28.5 µm | 4.1 µm |
| **Fused model** | 1.8 µm | 0.10 µm | 12.7 µm | 1.2 µm |

### 3.2 Actual measurement

Actual measurements on two different kinds of freeform surfaces are presented to further examine the performance of the proposed method. A sinusoidal structured surface defined by Eq. (20) has been machined and is measured by Zygo Nextview optical profiler, as shown in Fig. 5.

$$z = 0.015 * \left( \sin(15x) + \cos(15y) \right) \tag{21}$$

The workpiece was measured by 5.5x and 20x objectives in two steps to fully capture the geometric information. The two datasets are considered possessing approximately same level of uncertainties according to the specifications of the instrument. However they possess different resolutions and are embedded in different coordinate frames, which require data fusion method to generate unique representation of the surface. The proposed method is used to fuse the datasets which are measured by two different objectives.

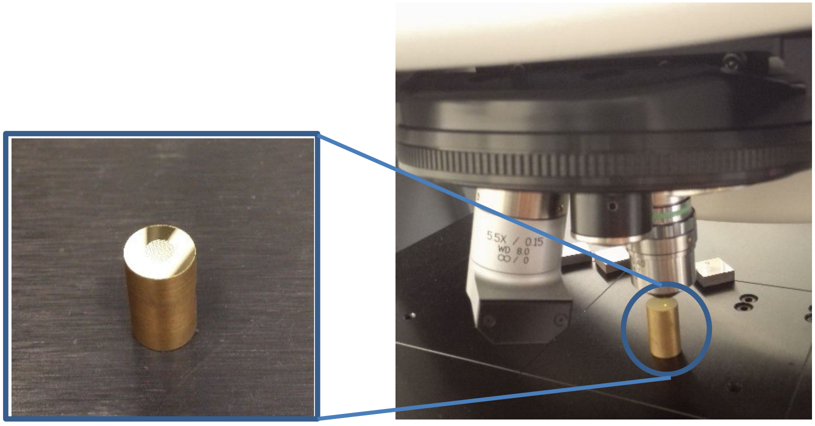


Fig. 5: Measurement of a sinusoidal structured surface on optical profiler

It starts from transforming the dataset captured by 20x objectives to the coordinate frame of the dataset captured by 5.5x objective based on the proposed intrinsic surface feature based data registration method. The overlapping area of the two datasets is then identified and is fused using the proposed weighted least square based method. Firstly, the B-spline model of the dataset captured by 5.5x objective is constructed. The generated knot vector is used as initial condition to construct the B-spline model of the dataset captured by 20x objective. Secondly, the generated basis functions are then used to establish the fusion system. The fused model is then used to evaluate the form error of the measured surface based best fitting method [16]. Fig. 6 shows the form error evaluation process. The result is also compared with that are obtained by the original two measured datasets. The RMS error of the measured surface are identified to be 0.102 μm, 0.097 μm, and 0.085 μm by 5.5x, 20x, and fusion dataset, respectively. It is noted that the fusion dataset possesses improved accuracy than both two measured datasets.

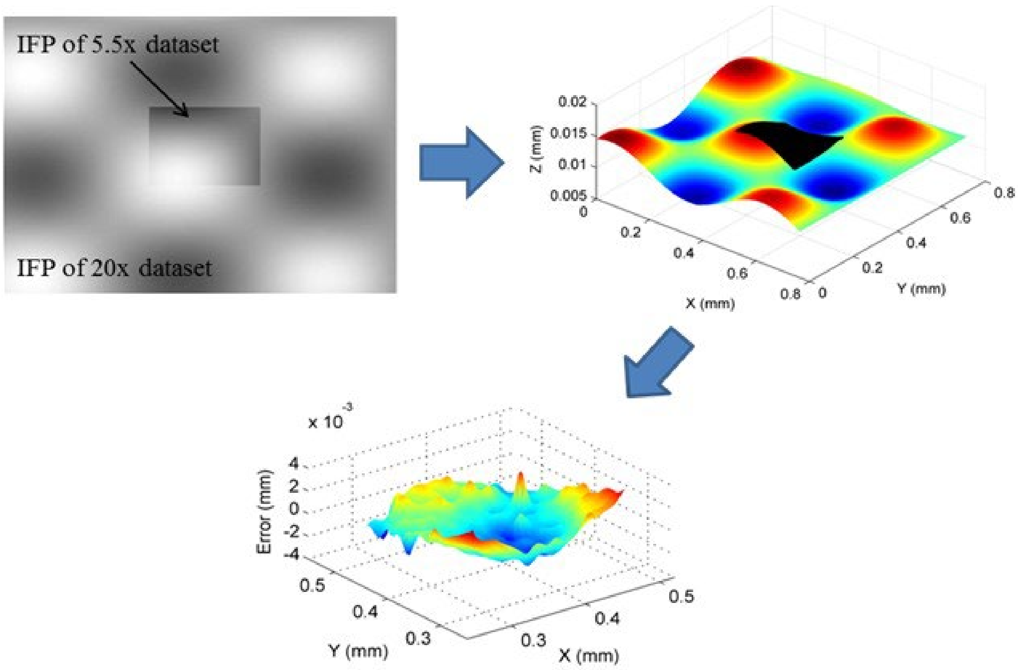


Fig. 6: Form error evaluation of the measured freeform surface

Another case study was conducted on a more complicated surface which is generated by superimposing sinusoidal waves on a parabola as defined by Eq. (22).

$$z = -0.01x^2 - 0.01y^2 + 0.015\cos(2y) + +0.015\cos(2y) \qquad (22)$$

where $x, y \in [-10, 10]$mm. To perform both high efficiency and high accuracy, two kinds of different measurement instruments including a high precision CMM and a Keyence LK-laser scanner are cooperatively used to measure the surface. Fig.7 shows the measurement of the machined surface on a CMM. The uncertainty of the laser scanner is identified to be u=3.4μm (1σ, normal) by a reference ball. The CMM possesses length measurement uncertainty with U=(0.6+L/500, L in mm) µm, and the probing error with u=0.9µm (1σ, normal).

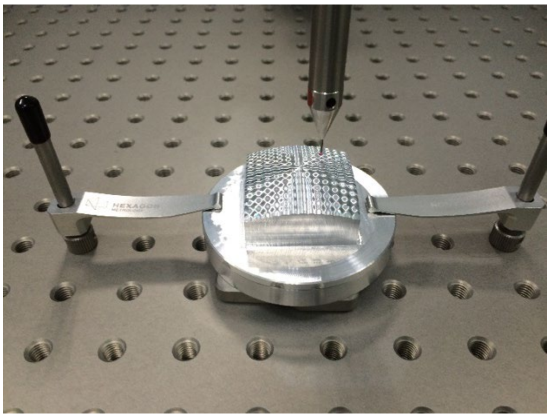

Fig. 7: Measurement of a multi-scaled complex surface

The measurement has been conducted in two steps. In the first step, CMM is used to measure the workpiece with 0.5 mm spacing. A total of 1600 points were measured with uniform sampling over the entire surface. Secondly, the laser scanner was used to measure the workpiece. Approximately 10000 points were uniformly sampled with spacing 0.2mm in both X and Y direction.

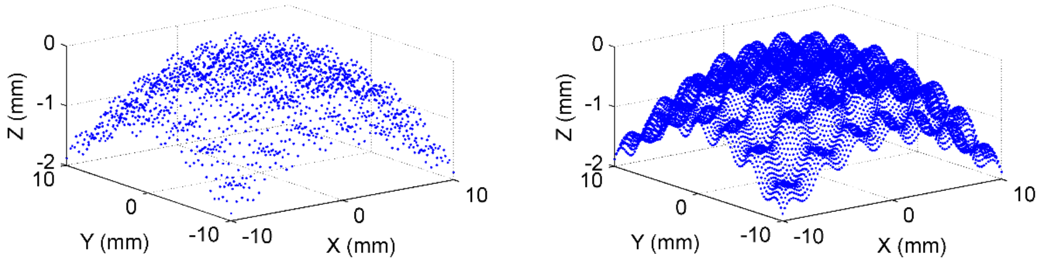


(a) CMM measured dataset (b) laser scanner measured dataset

Fig. 8: Measured datasets by CMM and laser scanner

The two datasets possess different resolutions and different levels of associated uncertainties and are embedded in different coordinate frames. The proposed method is then used to perform the multi-sensor data fusion. Fig. 9 shows the established fused surface model and the evaluated form error. The results are also compared with that is obtained by the original measured datasets, as summarized in Table 2. It is seen from the results that the form error evaluated by the dataset measured by CMM possesses highest error than the others. This is due to the insufficient sampling of the workpiece which leads to large error in representing the form of the surface. It is noted from the comparison that the fusion dataset possesses better results than both the two datasets in evaluating the form error of the workpiece. This demonstrates the capability of the proposed method in fusing multi-sensor datasets which have complex geometry.

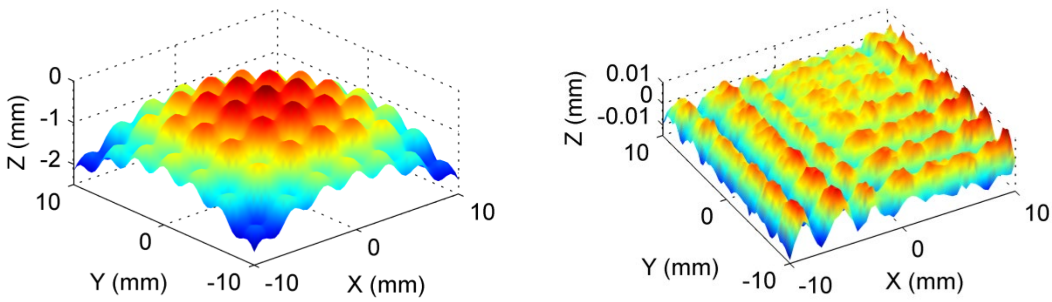


(a) Reconstructed surface (b) evaluated form error

Fig. 9: Reconstructed measured surface and the evaluated form error

Table 2: A summary of the evaluated form error

| | **CMM dataset** | **Laser dataset** | **Fused model** |
|---|---|---|---|
| **PV** | 20.6 µm | 17.9 µm | 13.1 µm |

| | | | |
|---|---|---|---|
| **RMS** | 2.6 μm | 2.8 μm | 2.4 μm |

## 4. Conclusion

This paper presents a data fusion method for measurement of freeform surfaces on multi-sensor systems. To address the key issues in multi-sensor data fusion, two algorithms were presented, including intrinsic feature based data registration and B-spline based weighted least square data fusion. A theoretical analysis of the uncertainty propagation in data fusion process is also given in detail. Both computer simulation and actual measurement has been conducted to examine the validity of the proposed method. The results imply that the proposed fusion method is capable of improving the fidelity of the reconstructed surface model via weighted fusion process.

## Acknowledgement

The work was supported by the National Natural Science Foundation of China (No. 51505404), China National Program on Key Basic Research Project (No. 2011CB013203) and the Research Grants Council of the Government of the Hong Kong Special Administrative Region, China under the project No. PolyU 152028/14E. The work was also supported by a PhD studentship (project account code: RTHC) from The Hong Kong Polytechnic University.

## Reference

[1] Fang FZ, Zhang XD, Weckenmann A, Zhang GX, Evans C, Manufacturing and measurement of freeform optics. CIRP Ann-Manuf Tech 2013; 62; 823-46.

[2] Jiang X, Whitehouse DJ, Technological shifts in surface metrology. CIRP Ann-Manuf Tech 2012; 61; 815-36.

[3] Whitehouse DJ, Surface geometry, miniaturization and metrology. Phil Trans R Soc A 2012; 370; 4042-65.

[4] Wang J, Leach R, Jiang X, Review of the mathematical foundations of data fusion techniques in surface metrology. Surf Topogr: Metrol Prop2015; 3; 023001.

[5] Savio E, Chiffre LD, Schmitt R, Metrology of freeform shaped parts. CIRP Ann-Manuf Tech 2007; 56; 810-35

[6] Hansen H, Carneiro K, Haitjema H, Chiffre L, Dimensional micro and nano metrology. CIRP Ann-Manuf Tech 2006; 55; 721-43

[7] Leach R, Boyd R, Burke T, Danzebrink HU, Dirscherl K, Dziomba T, Gee M, Koenders L, Morazzani V, Pidduck A, Roy D, Unger WE, Yacoot A, The European nanometrology landscape. Nanotechnology 2011, 22; 062001.

[8] Weckenmann A, Peggs G, Hoffmann J, Probing systems for dimensional micro- and nano-metrology. Meas Sci Tech 2006; 17; 504-9.

[9] Weckenmann A, Jiang X, Sommer K, Newschaefer-Rube U, Seewig J, Shaw L, Estler T, Multisensor data fusion in dimensional metrology, CIRP Ann-Manuf Tech 2009; 58; 701-21.

[10] http://www.werthmesstechnik.de. Accessed in 8 Apr 2016.

[11] Ramasamy SK, Multi-scale data fusion for surface metrology. PhD thesis, the University of North Carolina at Charlotte USA, 2011.

[12] Besl PJ, McKay ND, A method for registration of 3D shapes", IEEE T Pattern Anal 1992; 14; 239-56.

[13] Li Y, Gu P, Free-form surface inspection techniques state of the art. Comput- Aided Des 2004; 36; 1395-417.

[14] Sharp GC, Lee SW, Wehe DK, ICP Registration using invariant features. IEEE T Pattern Anal 2002; 24; 90-102.

[15] Ren MJ, Cheung CF, Kong LB, Jiang J, Invariant feature pattern based form characterization for the measurement of ultra-precision freeform surfaces. IEEE T Instrum Meas 2012; 61; 963-73.

[16] Zhu KP, Wong YS, Lu WF, Fuh JY, A diffusion wavelet approach for 3D model matching. Comput-Aided Des 2009; 41; 28-36.

[17] Ramasamy S K, Raja J, Boudreau BD, Data Fusion Strategy for Multiscale Surface Measurements. Journal of Micro and Nano-Manufacturing 2013; 1; 011004.

[18] Colosimo BM, Pacella M, Senin N, Multi-sensor data fusion via Gaussian process models for dimensional and geometric verification. Precis Eng 2015; 40; 199-213.

[19] Qian ZG, Wu CF, Bayesian hierarchical modeling for integrating low-accuracy and high-accuracy experiments. Technometrics 2012; 50; 192-204.

[20] Forbes AB, Weighting observations from multi-sensor coordinate measuring systems. Meas Sci Technol 2012; 23; 025004.

[21] Thacker NA, Lacey AJ, Tutorial: The likelihood interpretation of the Kalman filter. University of Manchester, UK, 2006.

[22] Besl PJ, Surface in range image understanding. New York: Springer-Verlag, 1988.

[23] Wang CC, Tang K, Yeung ML, Freeform surface flattening based on fitting a woven mesh model. Comput-Aided Des 2005; 37; 799-814.

[24] Chen Q, Defrise M, Deconinck F, Symmetric Phase-only matched Filtering of Fourier-Mellin Transforms for Image Registration and Recognition. IEEE T Pattern Anal 1994; 16; 1156-68.

[25] Kalogerakis E, Simari P, Nowrouzezahrai D, Singh K, Robust statistical estimation of curvature on discretized surfaces. In Eurographics Symposium on Geometric Processing 2007, 13-22.

[26] Piegl L, Tiller W, The NURBS book. Berlin: Springer-Verlag, 1997.

[27] Ren MJ., Cheung CF., and Kong LB, A robust surface fitting and reconstruction algorithm for form characterization of ultra-precision freeform surfaces. Measurement 2011; 44; 2068-77.